Structural and optical behavior of Y_2O_3 nanocrystallites synthesized by sol-gel technique

Rachna Ahlawat*

Department of Physics, Materials Science Lab., Ch. Devi Lal University, Sirsa 125055, Haryana, India

*Corresponding author; E-mail: rachnaahlawat2003@yahoo.com

Received: 29 March 2016, Revised: 24 September 2016 and Accepted: 19 April 2017

DOI: 10.5185/amp.2017/631
www.vbripress.com/amp

Abstract

Y_2O_3 nanocrystallite has been successfully synthesized by sol-gel technique. $Y(NO_3)_3.4H_2O$ and TEOS were used as precursors and obtained powdered form of the oxide. In this study, stepwise annealing process has been performed and obtained almost spherical Y_2O_3 nanocrystallites. As-prepared sample was annealed at 900°C and their comparison has been studied in detail. Structural investigations of the prepared nanocrystallites were carried out by XRD and TEM. Optical behavior of the sample was investigated using UV-Vis absorption spectra. Also, band gap energy Eg = 5.9 eV has been calculated using Tauc's plot. It is expected that the studies of these phenomena would open a new vistas of energy conversion devices and high speed optoelectronic instrumentation. Copyright © 2017 VBRI Press.

Keywords: Yttrium oxide, sol-gel technique, X-ray diffraction, TEM, band gap energy.

Introduction

The synthesis of functional nanomaterials is still a challenge in the field of nanotechnology and comprises a major body of research in this field. Nanocrystalline materials with tailored structural and optical properties are expected to have a great technological importance **[1]**. Yttria (Y_2O_3) has recently attracted much attention because of several properties, such as its crystallographic stability, high mechanical strength, high thermal conductivity, large optical band gap, a relatively high dielectric constant in the range, a rather high refractive index **[2-3]**. As a well-known phosphor host material, yttria has been used in cathode radiation tube (CRT), field emission display (FED), and thin film electroluminescence (TFEL) devices **[4]**.

There are various methods developed to synthesize nanocrystallites, either in a stand-alone form or inside a host matrix. Yttria nanocrystallites can be synthesized by different methods such as sol–gel, hydrothermal, and combustion synthesis **[5-6]**. The sol-gel process combines the advantage of lower temperature and possibility of making of finely dispersed powders with ease and low cost. Xiaoyi *et al* **[7]** used co-precipitation technique to synthesize Y_2O_3/SiO_2 core shell structure and studied their optical properties. Also, Liu et al. **[8]** have studied tunable silica shell and its modification on photoluminescent properties of $Y_2O_3:Eu^{3+}@$ SiO_2 nanocomposites. The dependences of PL properties of $Y_2O_3:Eu^{3+}$ on the thickness of the silica shell and excitation power density were systemically studied under charge transfer excitation (254 nm) and 7FJ-5D2 inner-shell excitation (460-486 nm). Cannas *et al* **[9]** used sol-gel method to prepare $Y_2O_3:SiO_2$ powder T~ 900°C & 1300°C (0.5 h). They found that at moderate temperature sintered $Y_2O_3:SiO_2$ was amorphous. In the present study, sol-gel synthesis route and importance of stepwise annealing has been discussed in detail for preparation of Y_2O_3 nanocrystallite. Structural characterizations were carried out by XRD and TEM. Also, the optical properties were examined using UV-Vis absorption spectrum and calculated their band gap energy.

Experimental

Materials

Yttrium nitrate tetra hydrate, hydrochloric acid, tetraethoxysilane (TEOS) and nitric acid were supplied by Sigma Aldrich, U. S. with 99.999 % purity and ethanol was supplied by Merck & Co., U. S., with 99.9 % purity.

Synthesis of Y_2O_3 nanocrystallites

Based on our previous studies **[10-11]**, to prepare the samples molar ratio of starting solution was taken as 2.30**:**0.72**:**0.29**:**0.027 for H_2O: C_2H_5OH: HCl: TEOS. 2.2 wt % $Y(NO_3)_3.4H_2O$ was introduced in the pre-hydrolyzed solution under heating. The prepared gel was kept at room temperature for 21 days for aging of the samples. After aging, the samples were further dried at

100°C for 24 hours and dried samples were powered by pestal-motrar. The powder sample was annealed in muffle furnace (KSL 1600X, MTI) in air. The dried sample is named as-prepared (a) and annealed sample as (b) which are also given below:

(a) As -prepared (dried at 100°C for 24 hours in air)

(b) $R_T \xrightarrow{6C/min}$ 250°C (3h) $\xrightarrow{5C/min}$ 500°C (3h) $\xrightarrow{4C/min}$ 750°C (3h) $\xrightarrow{2C/min}$ 900°C (6h)

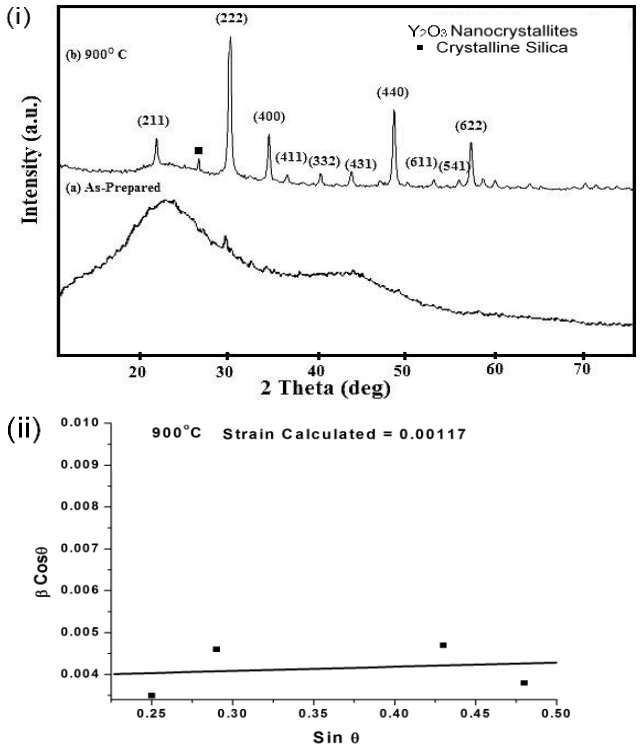

Fig. 1. (i) XRD pattern of Y_2O_3 nanocrystallites (ii) W-H plot for annealed sample (b).

Characterizations

The prepared samples were characterized by X'pert Pro X-Ray Diffractometer with Cu-kα1 radiation in the range of 5° - 80° in steps of 0.017° (40 mA, 45 KV) for the determination of crystalline structure of samples which were further confirmed by HRTEM Hitachi 4500 micrograph (Tokyo, Japan). Specimens for TEM were prepared by dispersing the powder sample in ethanol and placed a droplet of suspension on a grid coated with perforated carbon. Absorption spectra of the samples were observed with the help of Lambda 750 (Perkin Elmer, Shelton, CT) spectrophotometer in the wavelength range 200–600 nm.

Results and discussion

XRD analysis

Fig. 1 illustrates the X-ray diffraction (XRD) patterns of as-prepared and annealed sample of Y_2O_3 nanocrystallite.

The diffractogram of as-prepared sample shows amorphous nature of the precursors. A broad diffraction hump around 2θ ~ 22.8° with a sharp peak at 2θ ~ 29.64° has been observed, which indicates the amorphous nature of SiO_2 matrix although Y_2O_3 is mixed properly into gel. In order to study the effect of stepwise annealing, the sample was heated up to 900°C and for 6h with different ramp rates at different steps of temperature.

Diffraction pattern (b) infers the pure cubic phase of Y_2O_3 crystalline structure having the characteristic peak of at 2θ ~ 29.25° along with some weaker peaks between 2θ ~ 20° - 60°. To identify complete structure of the prepared powder, these peaks are assigned Miller indices respectively (details are given in **Table 1**) having lattice parameter a = 10.56 Å and space group Ia3. Moreover, code was also confirmed by comparing the obtained Check cell data with the JCPDS card no. 41-1105 **[6]**.

Table 1. Detail of the XRD parameters and (hkl) planes.

Pos. [°2Th.]	FWHM [°2Th.]	d-spacing [Å]	Rel. Int. [%]	Area [cts*°2Th.]	Miller Indices [hkl]
20.6804	0.1673	4.29509	12.09	31.75	(211)
25.6554	0.1506	3.47238	5.63	13.29	Silica
29.2748	0.2509	3.05078	100.00	393.89	(222)
33.9198	0.2007	2.64289	22.16	69.83	(400)
36.0254	0.2342	2.49310	3.81	14.00	(411)
39.9980	0.2342	2.25418	5.55	20.41	(332)
43.6955	0.2007	2.07162	6.38	20.11	(431)
48.6729	0.3011	1.87078	35.22	166.49	(440)
53.3702	0.3011	1.71668	3.35	15.86	(611)
56.3242	0.3346	1.63345	3.38	17.74	(541)
57.7194	0.2676	1.59725	21.17	88.95	(622)

On further inspection, a small peak has been observed at 2θ ~ 25.64° which strengthen the crystalline phase of silica **[10]**. These results manifest that pure cubic phase of yttrium oxide could be obtained at moderate temperature (900°C) by stepwise annealing of the sample. Thus, the size and shape of Y_2O_3 nanocrystallites using sol gel method can be tailored by varying ramp rates and incubation times.

Calculation of micro strain and crystallite size

The strain and crystallite size produces peak broadening in the diffraction pattern. The sample annealed at 900°C is well crystalline and single phase (cubic phase), therefore the crystallite size and strain for the sample (b) was calculated using W-H method **[12]**. The W-H equation is:

$$\beta \cos\theta = \frac{k\lambda}{D} + 2\epsilon \sin\theta \qquad (1)$$

where K is the shape factor which is 0.9 for uniform small size crystals, λ is the wavelength of X-ray, θ_{hkl} is the Bragg angle, β_{hkl} is the FWHM, ε is the strain and d is an average crystalline size measured in a direction perpendicular to the surface of the specimen. The graph is plotted between sin $_{hkl}$ and β_{hkl} Cos θ_{hkl} as shown in the **Fig. 1(ii)**. The lattice strain was calculated using the slope of the straight line which has negligible value ~1.17 10^{-3}. Williamson-Hall relation reduces to be well known

Debye-Scherer's equation under the considerations of zero micro strain, = 0 in equation (1). Therefore,

$$D = \frac{K\lambda}{\beta \cos\theta} \quad (2)$$

where the symbols have their usual meanings. The average size (*D*) of nanocrystallite was calculated for the sample (b) using equation (1) & (2) and it was found to be ~ 35 & 33 nm, respectively.

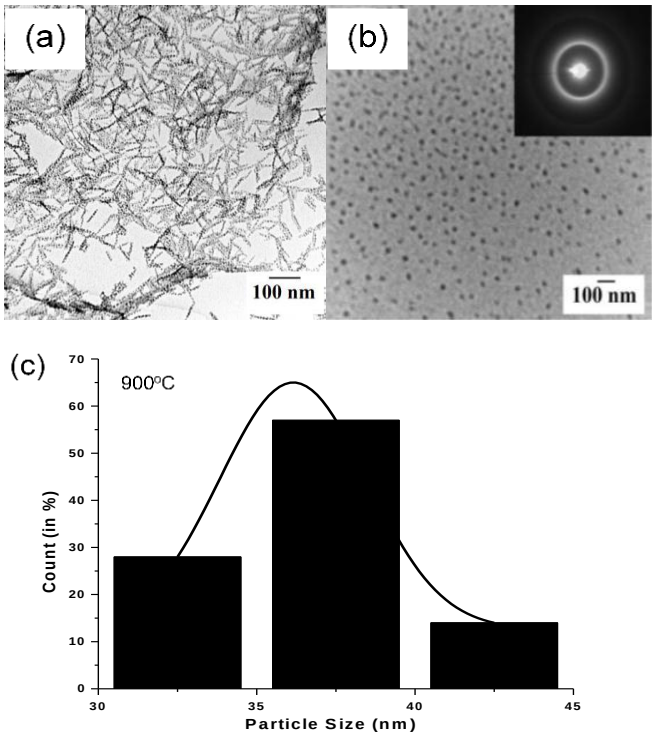

Fig. 2. TEM micrograph of Y_2O_3 nanocrystallites (a) as-prepared, (b) annealed at 900°C, and (c) particle size distribution.

TEM analysis

It is necessary to obtain the particle size and the information about the nanostructure by direct measurement such as transmission electron microscope (TEM) which can reveal the size and morphology of the particle. **Fig. 2** shows TEM micrograph of as-prepared sample (a) the annealed sample (b). The selected-area electron-diffraction (SAED) pattern of the individual nanocrystallite was also obtained to indicate the formation of the cubic structure and crystalline nature of the particles (inset of **Fig. 2(b)**) As expected, micrograph of sample (a) shows typical chain-like structure of acidic gel of precursors and confirms the amorphous nature of the same sample. TEM image of the sample (b) shows non-agglomerated nanocrystallites of spherical shape having size ranges 30 - 45 nm (~ 37 nm). The particle size distribution of this sample shows that nanocrystallites of Y_2O_3 have narrow grain size distribution within the silica matrix as shown in the **Fig. 2(c)**. Moreover, the histogram (c) indicated that nearly 80 % nanocrystallites are having size ranges 30 - 40 nm.

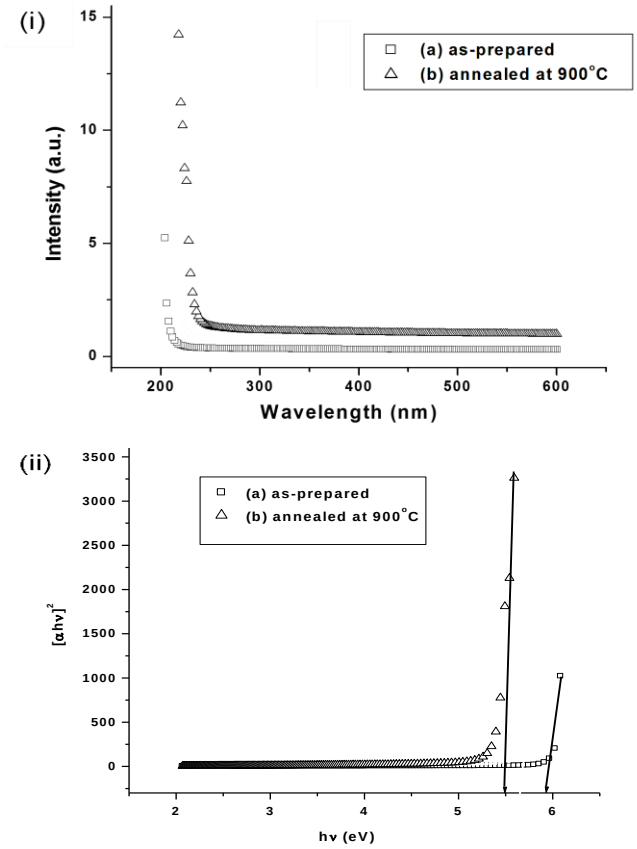

Fig. 3. (i) Absorption spectra (ii) Band gap energy of Y2O3 nanocrystallites.

Optical absorption and band gap

The optical absorption spectra of the samples are shown in **Fig. 3(i)** and the absorption peak appears in the range of 200-220 nm. It is also observed that the peak shift is appeared towards higher wavelength side for the annealed sample (b). The shift in the absorption peak position of the as-prepared and annealed sample evidently point out the size dependence of the nanocrystallites powder. The shift in the absorption peak position of the as-prepared and annealed sample evidently point out the size dependence of the nanocrystallites powder. The optical properties of the Y_2O_3 nanocrystallites dispersed in silica matrix were identical to the Y_2O_3 powder **[5, 7]**.

The peak positions also reflect the band gap energy of the prepared nanocomposite. The relation between the incident photon energy ($h\nu$) and the absorption coefficient (α) is given by the following relation:

$$(Ah\nu)^{\frac{1}{n}} = A(h\nu - E_g) \quad (3)$$

where A is constant and E_g is the band gap energy of the material and the exponent n depends on the type of transition. For direct allowed transition n = 1/2, for indirect transition n = 2, for direct forbidden n = 3/2 and for indirect forbidden n = 3. Band gap energy of the samples were calculated by plotting $(\alpha h\nu)^2$ verses $h\nu$ and then extrapolating the straight portion of the curve on $h\nu$ axis at $\alpha = 0$ as shown in the **Fig. 3(ii)** and found to be 5.5 and 5.9 eV for the sample (a) & (b), respectively.

Conclusion

Y_2O_3 nanocrystallites in silica matrix have been successfully synthesized by sol-gel technique with an average size of ~ 35 nm. The cubic phase of yttria nanocrystallites is confirmed with XRD and TEM results. XRD and TEM studies confirm that stepwise heat treatment results in almost spherical nanocrystallites of Y_2O_3. The observed absorption peak for annealed sample has been shifted towards higher wavelength side. Band gap energy has been calculated as 5.9 eV for the annealed sample. It is felt deeply by the author that the work will be of basic importance for the better understanding of the mechanisms of photonic devices, catalytic system including laser, opto-and micro-electronic and optical fiber, etc.

References

1. Cao, G.; Nanostructures & Nanomaterials, Synthesis, Properties & Applications, London, Imperial College Press, **2004.**
   DOI: 10.1504/IJMMP.2008.022045
2. Yao, G.; Su, L. B.; Xu, J.; Xu, X. D.; Zheng, L. H.; Cheng, Y.; *J. Cryst. Growth.*, **2008**, *310*, 404.
   DOI: 10.1016/j.jcrysgro.2007.10.032
3. Jordan, E. H.; Gell, M.; *J. Am. Ceram. Soc.*, **2013**, *96*, 346.
   DOI: 10.1111/jace.12123
4. Kitai, A. H.; *Thin Solid Films*, **2003**, *445*, 367.
   DOI: 10.1016/S0040-6090(03)01187-8
5. Srinivasan, R.; Arumugam, Y.; Bose, C.; *Materials Research Bulletin*, **2010**, *45*, 1165.
   DOI: 10.1016/j.materresbull.2010.05.020
6. Ahlawat, R.; *Cera. Int.*, **2015**, *41*, 7345.
   DOI: 10.1016/j.ceramint.2015.02.035
7. Xiaoyi, S.; Yuchun, Z.; *Rare Met*, **2011**, *30*, 33.
   DOI: 10.1007/s12598-011-0192-x
8. Liu, T.; Xu, W.; Bai, X.; Song, H.; *J. Appl. Phys*., **2012**, *111*, 064312.
   DOI: 0.1063/1.3694767
9. Cannas, C.; Casu, M.; Lai, A.; Musinu, A.; Piccaluga, G.; *Phys. Chem. Chem. Phys.* **2002**, ***4***, 2286.
   DOI: 10.1039/B110996K
10. Ahlawat, R.; Aghamkar, P.; *Acta Phys. Pol. A*, **2014,** *126*, 736.
    DOI: 10.12693/APhysPolA.126.736
11. Ahlawat, R.; *Int. J. Appl. Ceram. Technol.*, **2014**, 1
    DOI: 10.1111/ijac.12343
12. Tan, S. T.; Chen, B. J.; Sun, X. W.; Fan, W. J.; Kwok, H. S.; Zhang, X. H.; Chua, S. J.; *J. Appl. Phys.*, **2005**, *98*, 013505.
    DOI: 10.1063/1.1940137

